Mechanisms regulating tissue-specific polarity of monocarboxylate transporters and their chaperone CD147 in kidney and retinal epithelia

Ami A. Deora*, Nancy Philp†‡, Jane Hu§, Dean Bok§¶‖, and Enrique Rodriguez-Boulan*‡

*Margaret M. Dyson Vision Research Institute, Weill Medical College of Cornell University, New York, NY 10021; †Department of Pathology, Anatomy and Cell Biology, Thomas Jefferson University, Philadelphia, PA 19107; and §Jules Stein Eye Institute, ¶Brain Research Institute, and ‖Department of Neurobiology, School of Medicine, University of California, Los Angeles, CA 90095

Edited by David D. Sabatini, New York University School of Medicine, New York, NY, and approved September 22, 2005 (received for review May 27, 2005)

Proton-coupled monocarboxylate transporters (MCT) MCT1, MCT3, and MCT4 form heterodimeric complexes with the cell surface glycoprotein CD147 and exhibit tissue-specific polarized distributions that are essential for maintaining lactate and pH homeostasis. In the parenchymal epithelia of kidney, thyroid, and liver, MCT/CD147 heterocomplexes are localized in the basolateral membrane where they transport lactate out of or into the cell depending on metabolic conditions. A unique distribution of lactate transporters is found in the retinal pigment epithelium (RPE), which regulates lactate levels of the outer retina. In RPE, MCT1/CD147 is polarized to the apical membrane and MCT3/CD147 to the basolateral membrane. The mechanisms responsible for tissue-specific polarized distribution of MCTs are unknown. Here, we demonstrate that CD147 carries sorting information for polarized targeting of the MCT1/CD147 hetero-complexes in kidney and RPE cells. In contrast, MCT3 and MCT4 harbor dominant sorting information that cotargets CD147 to the basolateral membrane in both epithelia. RNA interference experiments show that MCT1 promotes CD147 maturation. Our results open a unique paradigm to study the molecular basis of tissue-specific polarity.

apical | basolateral | polarized epithelium

Extensive research has identified apical and basolateral sorting signals that control polarized plasma membrane protein localization in epithelial cells (reviewed in refs. 1–3). Apical sorting signals include glycosylphosphatidylinositol anchors, O-glycans, N-glycans, and protein sequences in either transmembrane or cytoplasmic domains. Basolateral signals include Tyr, di-Leu, single Leu, and di-hydrophobic consensus motifs present in the cytoplasmic domain of the protein. However, most of these studies have focused on proteins with just one transmembrane domain. Very little is known about the mechanisms that regulate the polarized distribution of many key metabolite transporters that, like P-type ATPases, anion, monocarboxylate, and L-amino acid transporters, are multispan nonglycosylated proteins. Many of these metabolite transporters require dimerization with a single span type I or II glycoprotein for surface expression (4–9). Only in the case of Na^+,K^+-ATPase and H^+,K^+-ATPase it is known that sorting information for polarized delivery is present in the nonglycosylated, catalytic α-subunit (4). For no other metabolite transporter is this information available, despite their crucial polarized transport roles in different epithelia.

Monocarboxylate transporters (MCTs) are nonglycosylated multispan proteins with 12 predicted transmembrane domains and cytoplasmic N- and C-terminal ends (6, 10–14). Of 14 known family members, only MCT1–MCT4 are well characterized; they share 40–60% homology and have distinct tissue distribution and lactate/proton transport kinetics (15, 16). MCT1, MCT3, and MCT4 associate with CD147 (9, 12, 17), a ubiquitous type I single-span transmembrane glycoprotein of the Ig superfamily (18). MCT2 was recently found to associate with GP70, a homolog of CD147 (19). Coexpression studies in cultured cells suggest that CD147 is required for delivery of MCT1 and MCT4 to the plasma membrane (12). Furthermore, CD147 knockout mice fail to express MCT1, MCT3, and MCT4 in retinal cells, even when their mRNAs are present (9).

Lactic acid plays a key role in the nutrition of tissues like retina, brain, heart, and fast-twitch muscle fibers (6, 20, 21). In the retina, lactate is a major nutrient for rods and cones and reaches a concentration 10 times higher than in blood upon production by Müller cells (22). Knockout mice for the MCT chaperone CD147 exhibit physiological and morphological alterations of the retina (23, 24). Retinal lactate levels are regulated by the retinal pigment epithelium (the blood–retinal barrier for the outer retina) via apically localized MCT1 (6, 10, 25) and basolaterally localized MCT3 (25, 26). A third member of the MCT family, MCT4, is normally not expressed in adult retinal pigment epithelium (RPE) but is expressed basolaterally in the human RPE cell line ARPE-19 (27). In contrast, MCT1 and MCT4 are expressed basolaterally in kidney tubules (ref. 16 and N.P., unpublished observation), and all three transporters are expressed basolaterally in the Madin–Darby canine kidney (MDCK) cell line (this work). The sorting signals in MCTs and the mechanisms responsible for their variable polarized localization in kidney and RPE cells are still unknown.

The MCT chaperone CD147 is basolaterally localized in most epithelia, including kidney epithelia and MDCK cells, but is present predominantly in the apical membranes of the RPE, with a smaller fraction at the basolateral membrane of this epithelium (9, 28, 29). Using extensive mutagenesis, we have identified a sorting signal consisting of Leu-252 in the C-terminal domain of CD147 that dictates its basolateral localization in MDCK cells (29) but is not recognized by RPE, resulting in a reversed apical localization of CD147 in this epithelium (28, 29). A crucial question emerges: Is the tissue-specific polarized localization of the MCT/CD147 hetero-complexes generated by the MCTs or by CD147? In the studies reported here, we developed an assay to answer this question. We overexpressed an apical mutant of CD147 (CD147-L252A) in MDCK cells to investigate whether CD147 or MCT1, MCT3, and MCT4 are responsible for polarized targeting of the heterocomplex. Our results indicate that the answer depends on the MCT. For MCT1/CD147 the dominant sorting information resides in CD147, whereas for MCT3/CD147 and MCT4/CD147 the dominant sorting information resides in the MCT transporter. Additional small interfering RNA (siRNA)-mediated knockout experiments demonstrated that MCT1 acts as a cochaperone for the maturation of CD147. Our findings significantly advance our understanding of the

CELL BIOLOGY

Conflict of interest statement: No conflicts declared.

This paper was submitted directly (Track II) to the PNAS office.

Abbreviations: MDCK, Madin–Darby canine kidney; RPE, retinal pigment epithelium; MCT, monocarboxylate transporter; Endo-H, endoglycosidase-H; LSCM, laser scanning confocal microscopy; siRNA, small interfering RNA; RNAi, RNA interference.

‡To whom correspondence may be addressed. E-mail: nancy.philp@jefferson.edu or boulan@med.cornell.edu.

mechanisms responsible for the tissue-specific localizations of MCT transporters in kidney and RPE and provide a unique paradigm to study the molecular bases of the so-called "flexible epithelial cell phenotype" (2).

Materials and Methods

Cell Culture. MDCK II cells and human fetal RPE cells were cultured as described in ref. 29. COS-7 cells were maintained in DMEM and 10% FBS. MDCK monolayers grown on Transwell polycarbonate filter units (0.4-μm pore size) (Costar) were used for surface biotinylation, lactate uptake, and immunofluorescence. Caco2 cells are epithelial cells derived from human colorectal adenocarcinoma. In our studies, we used a clone of Caco2 (C2BBE1) obtained from American Type Culture Collection. These cells were grown in DMEM supplemented with 10% FBS and 0.01 mg/ml transferrin (Sigma).

Site-Directed Mutagenesis of CD147. A QuikChange site-directed mutagenesis kit (Stratagene, La Jolla, CA) was used to introduce a point mutation of Leu to Ala (L252A) in the cytoplasmic domain of CD147 cDNA (Rat CE-9, GenBank accession no. X67215) in pcDNA3.1 vector (Invitrogen). The WT and L252A CD147 cDNAs were further used for point mutation of Glu to Ala (E221A) in the transmembrane domain of CD147. The pairs of custom-synthesized complementary mutagenic oligonucleotides were obtained from Sigma–Genosys (Woodlands, TX). All the constructs were subsequently sequenced to verify the intended mutation.

Immunofluorescence Microscopy. Cells were fixed in 4% freshly prepared paraformaldehyde in PBS for 20 min at room temperature and quenched with 50 mM NH_4Cl in PBS containing 1 mM $CaCl_2$ and 1 mM $MgCl_2$. Cryosections (8 μm) of human fetal RPE monolayers grown on filters were prepared and stained as described in ref. 27. The following primary Abs were used: mAb against the ectodomain of rat CD147 (RET-PE2 hybridoma, kindly provided by Colin Barnstable, Yale University, New Haven, CT), mouse anti-human CD147 (BD Biosciences), rabbit anti-GFP (Abcam, Cambridge, MA), and rabbit anti-Na^+,K^+-ATPase α-subunit (a kind gift from James Nelson, Stanford University, Stanford, CA). Isoform-specific peptide Abs were raised against MCT1, MCT3, and MCT4 as described in ref. 27. Anti-human MCT1 and anti-mouse MCT4 Abs crossreacted with MCT1 and MCT4 in MDCK cells. Secondary Abs used were Alexa Fluor 488-tagged anti-mouse IgG and Alexa Fluor 568-tagged anti-rabbit IgG. Immunostaining for CD147 was performed on nonpermeabilized cells followed by permeabilization with 0.1% Triton X-100 for immunostaining of MCTs. Images were obtained on a laser scanning confocal microscope (LSCM; Leica TCS SP2) with a $\times$63 oil objective. Serial (0.5 μm) *x–y* (*en face*) and *x–z* (top to bottom) sections were collected and processed with LCS software (Leica) and PHOTOSHOP 7.0 (Adobe Systems, San Jose, CA). Images presented here show confocal *x–y* and *x–z* sections.

pSuper Vector-Based siRNA. We silenced CD147 and MCT1 by using pSuper vector-based siRNA (30). pSuper vector was kindly provided by Reuven Agami (The Netherlands Cancer Institute, Amsterdam). Various siRNAs were constructed by cloning forward- and reverse-annealed sequences into the pSuper vector (see *Supporting Methods*, which is published as supporting information on the PNAS web site).

Human C2BBE1 cells were transiently transfected with the various pSuper vectors expressing siRNA by using the nucleofection system by Amaxa (Gaithersburg, MD). Cells were harvested for RNA isolation followed by RT-PCR, Western blot analysis, and metabolic pulse–chase analysis 72 h after transfection.

For detailed information on transfections, coimmunoprecipitation, domain-specific biotinylation, [^{14}C]L-lactic acid uptake, RT-PCR, Western blot analysis, and metabolic pulse–chase analysis, see *Supporting Methods*.

Results

CD147 Dictates Polarized Trafficking of the MCT1/CD147 Complex. MDCK cells express endogenous MCT1 at the basolateral membrane (data not shown). We isolated MDCK clones overexpressing CD147-WT and CD147-L252A or GFP-tagged versions of these proteins; the latter versions were used to facilitate resolution of the 50-kDa CD147 band from Ig chains in Western blots and to provide an alternative way to visualize CD147 distribution at the cell surface. The addition of C-terminal GFP did not alter the normal localization of CD147-WT or CD147-L252A. In all cases we were able to show quantitative coimmunoprecipitation of CD147-WT and CD147-L252A with endogenous canine MCT1 (Fig. 1*A*, shown is Western blot with GFP-tagged versions of the proteins). LSCM analysis indicated that CD147-WT and MCT1 localized basolaterally (Fig. 1*B Left*). Thus, overexpression of CD147-WT did not alter the basolateral polarity of MCT1. In striking contrast, MDCK clones expressing CD147-L252A localized this protein and MCT1 to the apical surface (Fig. 1*B Right*). Identical results were obtained with GFP-tagged versions of CD147 and CD147-L252A (Fig. 6, which is published as supporting information on the PNAS web site). Domain-selective cell-surface biotinylation (Fig. 1*C*) indicated that, although 90% of MCT1 was basolateral in MDCK cells expressing CD147-WT, 86% of MCT1 was apical in MDCK cells overexpressing CD147-L252A. As we have previously shown by using pulse–chase targeting assays that CD147-L252A is targeted directly to the apical domain (29), our results strongly suggest that the MCT1/CD147-L252A heterocomplex also follows a direct route from the Golgi complex to the apical domain. Because Abs against endogenous CD147 are not available, we were not able to determine the relative amounts of MCT1 associated with transfected and canine CD147. However, this ratio must be very high given that >80% of MCT1 changed from basolateral to apical upon overexpression of CD147-L252A. Control experiments indicated that overexpression of CD147-L252A did not change the basolateral localization of Na^+ K^+ ATPase (Fig. 7, which is published as supporting information on the PNAS web site) or Glut-1 (data not shown). Taken together, these results demonstrate that CD147 is the dominant partner that guides the polarized localization of the MCT1/CD147 lactate transport complex in MDCK cells.

Additional experiments showed that the apical MCT1/CD147-L252A complex was able to transport lactate (Fig. 1*D*). Whereas untransfected MDCK cells and MDCK cells overexpressing CD147-WT exhibited approximately two times higher lactate uptake from the basolateral side, MDCK cells overexpressing CD147-L252A showed 1.6-fold higher lactate uptake from the apical side. That this lactate uptake across basolateral and apical membranes was mediated by MCTs and not by simple diffusion was confirmed by its inhibition by the competitive inhibitor α-cyano-4-hydroxycinnamate (Fig. 1*D*) and by the correct lactate stereoisomer (L-lactic acid and not D-lactic acid, data not shown). Our assays confirm a previous report that polarized MDCK cells exhibit lactate influx preferentially from the basolateral membrane (31) and demonstrate that CD147-L252A promotes apical delivery of a functional MCT1.

MCT3 and MCT4 Dictate Basolateral Localization of the Heterocomplex in MDCK Cells. MDCK cells express a second member of the MCT family, MCT4, at the basolateral membrane (Fig. 2). Canine MCT4 coimmunoprecipitated with GFP-tagged rat CD147-WT and CD147-L252A as previously shown for MCT1 (Fig. 2*A*). This result is in agreement with previous published work that showed that MCT4 associates with CD147 and that in the CD147-null mouse MCT4 protein is not expressed in the neural retina (9, 12). LSCM demonstrated a basolateral localization of MCT4 in WT MDCK cells (data not shown) and in MDCK cells overexpressing GFP-

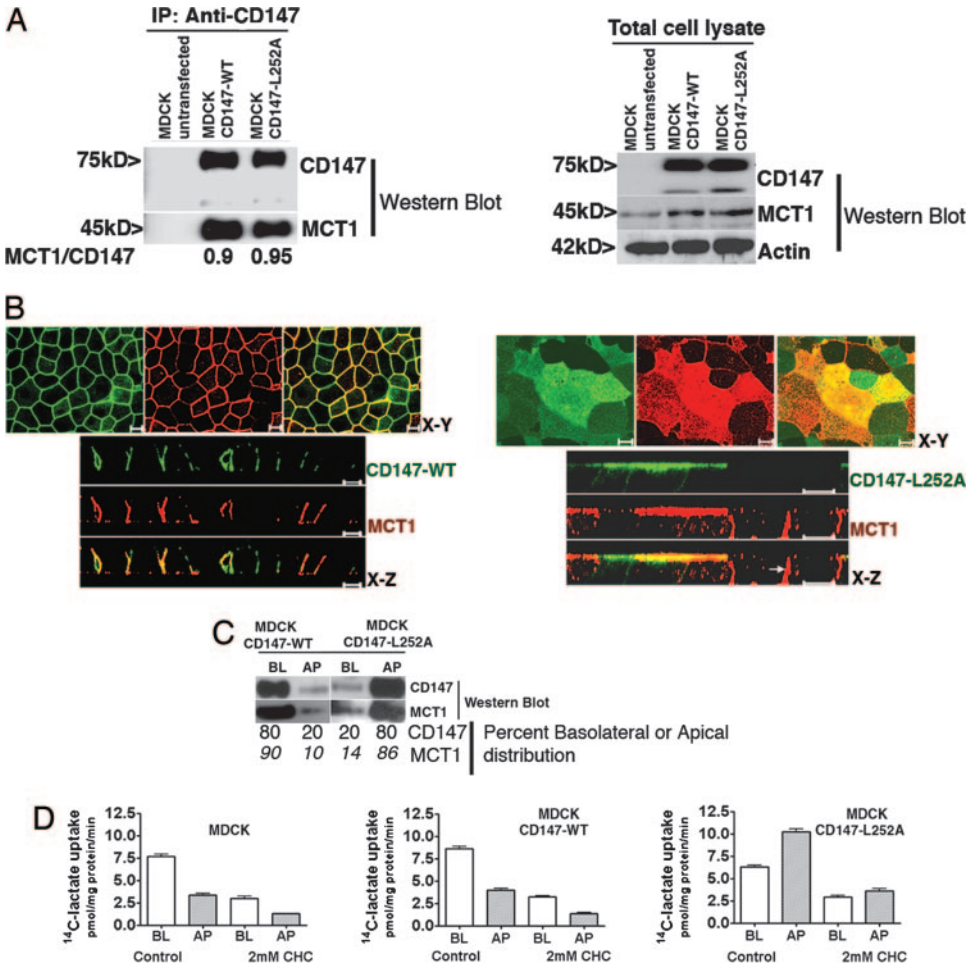

Fig. 1. Transfected rat CD147-L252A redirects endogenous MCT1 to the apical surface of MDCK cells. (*A*) Coimmunoprecipitation of CD147 and MCT1. The interaction between CD147 and MCT1 was studied by immunoprecipitation in MDCK cells stably transfected with CD147-WT-GFP or CD147-L252A-GFP, using an Ab against rat CD147 (RET-PE2). We used GFP-tagged CD147 for coimmunoprecipitation so that the Ab heavy chain would not mask the untagged 50-kDa CD147 band. Our previous studies have shown that a C-terminal GFP tag does not affect the trafficking of CD147 (29). The immunoprecipitate (*Left*) and the cell lysate (*Right*) were resolved by SDS/PAGE and Western blotted with CD147, MCT1, and β-actin Abs. The amounts of MCT1 interacting with either CD147-WT or CD147-L252A are similar. (*B*) LSCM analysis of clones of MDCK cells stably overexpressing CD147-WT (*Left*) or the apically targeted mutant CD147-L252A (*Right*). Shown are *x–y* and *x–z* projections of monolayers of MDCK cells immunostained for CD147-WT or CD147-L252A (green) and of endogenous MCT1 (red). Note that cells expressing CD147-L252A target endogenous MCT1 to the apical membrane; cells that expressed low or null levels of CD147-L252A targeted MCT1 basolaterally (*Right*; *x–z* section, arrow). (Scale bar, 10 μm.) (*C*) Domain-specific cell surface biotinylation was performed on MDCK cells expressing CD147-WT or CD147-L252A. After streptavidin-agarose precipitation, samples were analyzed by SDS/PAGE and Western blot. The results confirm that MDCK cells expressing CD147-L252A targets most of the (86%) endogenous MCT1 to the apical domain. (*D*) ^{14}C-lactate uptake was performed for 1 min in monolayers confluent on Transwells. WT MDCK and MDCK cells expressing CD147-WT exhibited two times higher lactate uptake on the basolateral side than on the apical side. In contrast, MDCK cells expressing CD147-L252A had a ^{14}C-lactate uptake 1.6-fold higher from the apical side. Hence, apically targeted MCT1 was functional. The MCT inhibitor α-cyano-4-hydroxycinnamate inhibited uptake by 60–70%. Data shown represent mean $\pm$ SD (n = 6). BL, basolateral; AP, apical.

tagged CD147-WT (Fig. 2*B Left*) or untagged CD147-WT (data not shown). However, in striking contrast with MCT1, the localization of MCT4 remained basolateral after overexpression of GFP-tagged CD147-L252A (Fig. 2*B Right*) or untagged CD147-L252A (data not shown), even when a major fraction of CD147-L252A was localized apically. A basolateral pool of CD147-L252A that colocalized with MCT4 was evident (Fig. 2*B Right*), suggesting that MCT4/CD147-L252A complexes were targeted to the basolateral membrane. Domain-selective biotinylation experiments confirmed quantitatively that the basolateral MCT4 distribution was not changed by overexpression of CD147-L252A (Fig. 2*C*). Additional experiments in COS cells demonstrated that CD147-L252A was as effective as CD147 in promoting surface delivery of MCT4, as previously shown for MCT4 and CD147-WT (12), indicating that the two proteins interact and confirming that the L252A mutation did not promote steric interference with the chaperone activity of CD147 (Fig. 8, which is published as supporting information on the PNAS web site). Taken together, our data strongly support the hypothesis that MCT4 carries dominant basolateral sorting information for localization of the MCT4/CD147 heterocomplex.

We carried out similar experiments with MCT3. Because MCT3 is not normally expressed by kidney cells, including MDCK cells, we transiently expressed human MCT3 in MDCK clones permanently overexpressing CD147-WT or CD147-L252A, using an electroporation protocol (Amaxa) that results in ≈50% of the cells expressing MCT3. Transfected human MCT3 coimmunoprecipitates with rat CD147-WT and CD147-L252A (Fig. 3*A*). As observed with MCT4, MCT3 localized basolaterally in MDCK clones overexpressing either CD147-WT or CD147-L252A (Fig. 3*B*), and a basolateral pool of CD147-L252A was detected predominantly in cells that expressed MCT3 (Fig. 3*B Right*). As reported above for MCT4, coexpression experiments in COS-7 cells demonstrated that MCT3 and CD147-L252A required each other for surface expression (Fig. 8), demonstrating that MCT3 interacts normally with CD147-L252A. Taken together, our data convincingly prove that CD147-L252A does form heterodimers with MCT1, MCT3, and MCT4 but is only capable of altering the polarized localization of MCT1. MCT3, like MCT4, appears to have strong intrinsic signals that mediate its basolateral localization in MDCK cells.

Mechanisms Underlying MCT Polarity in RPE. The results with MDCK cells provide additional tools to interpret the localization of MCTs and CD147 in RPE cells. Primary cultures of human fetal RPE show apical localization of CD147 and MCT1 and basolateral localization of MCT3 and a small fraction of CD147 (Fig. 4). Our observation is similar to what has been described in RPE *in situ* (6, 10, 14, 25, 26). Furthermore, the human RPE cell line ARPE-19 expresses CD147 and MCT1 at the apical membrane and MCT4 and CD147 at the basolateral membrane (ref. 27 and data not

CELL BIOLOGY

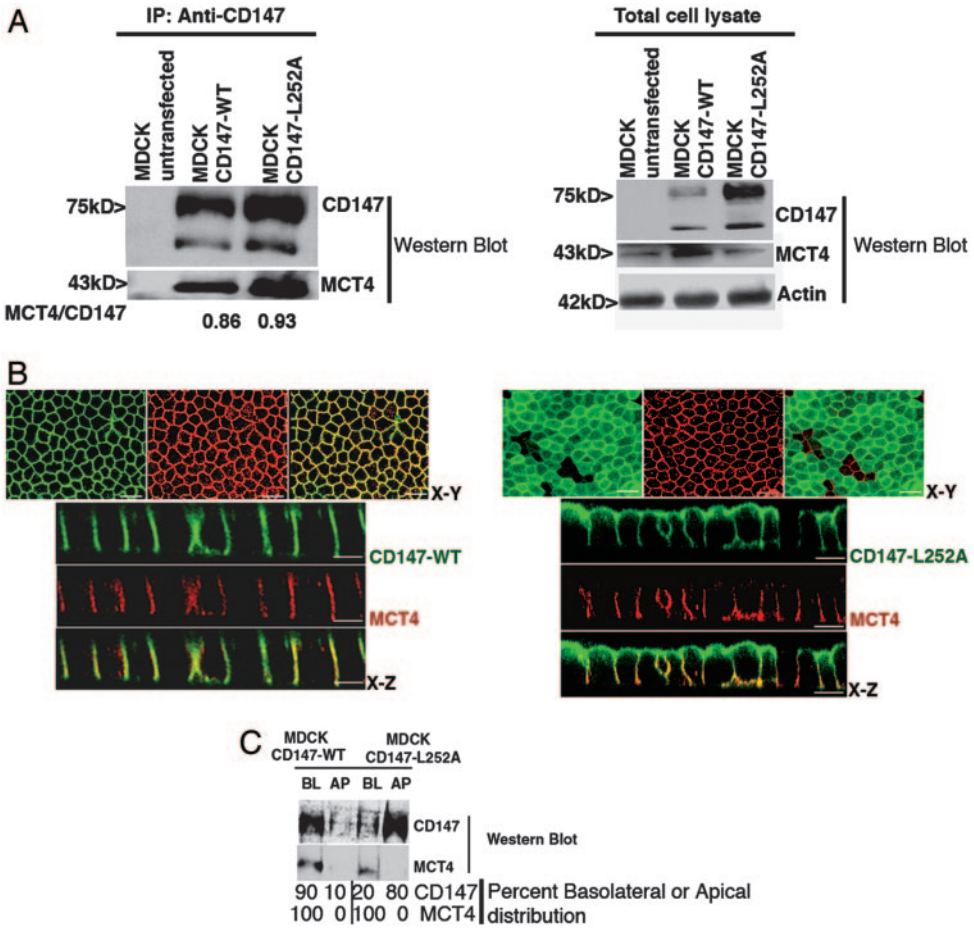

Fig. 2. CD147 does not control the polarized distribution of MCT4/CD147 complex. (*A*) Coimmunoprecipitation of CD147 and MCT4. The interaction of rat CD147-WT-GFP and CD147-L252A-GFP and canine MCT4 in MDCK was studied by coimmunoprecipitation with CD147 Ab and Western blotting in stably transfected MDCK cells. (*Right*) A Western blot of cell lysates is shown for comparison. (*Left*) Note that canine MCT4 coimmunoprecipitates with rat CD147-WT and CD147-L252A and the amount of MCT4 interacting with either of them is very similar. (*B*) LSCM analysis of clonal MDCK cell lines expressing CD147-WT-GFP (green) (*Left*) or CD147-L252A-GFP (green) (*Right*) were immunostained for endogenous MCT4 (red). *x–y* image represents maximum projection of the entire stack. (*Right*) Note that overexpression of apically targeted CD147-L252A did not affect the basolateral localization of MCT4. However, MCT4 colocalizes with the basolateral pool of CD147-L252A. (Scale bar, 10 μm.) (*C*) Domain-specific cell surface biotinylation followed by streptavidin-agarose pull down. Note that MCT4 is localized on the basolateral domain irrespective of the CD147 localization. BL, basolateral; AP, apical.

shown). Published data by our laboratory has shown that RPE cells do not recognize the basolateral signal of CD147 resulting in the targeting of this protein to the apical surface, probably driven by cryptic apical signals (28, 29). Together with these published data, the experiments in MDCK cells reported here suggest that the dominant sorting role of CD147 for MCT1 in MDCK cells is conserved in RPE leading to the apical localization of MCT1 in this epithelium. In contrast, the basolateral localization of MCT3 and MCT4 can be explained by the observation in MDCK cells that MCT3 and MCT4 are the dominant sorting partners in the heterocomplex they form with CD147.

A Candidate Glu Within the Transmembrane Domain of CD147 Is Not Critical for Control of MCT1 Polarity. The transmembrane domain of CD147 contains a highly conserved Glu residue (E221), which was suggested to be critical for association with MCTs and thus for plasma membrane delivery of the CD147/MCT complex (17). We carried out experiments to examine whether E221 was required for the trafficking interactions we detected between CD147 and MCT1. To this end, we mutated Glu to Ala (E221A) in CD147-WT and in CD147-L252A and investigated whether overexpression of these proteins resulted in changes in the localization of MCT1. As shown in Fig. 9, which is published as supporting information on the PNAS web site, CD147-E221A localized basolaterally and codistributed with MCT1 at the lateral membrane. Moreover, the double mutant CD147-L252A-E221A was targeted apically and was able to redistribute endogenous MCT1 to the apical membrane. These data suggest that E221 is not involved in interactions of CD147 with MCT1 and is not critical for membrane targeting of CD147 and MCT1, in contrast with a previous report (17). Additional work is necessary to elucidate the interacting domains of these two proteins required for their cotransport across the cell.

MCT1 Is Essential for Maturation of CD147. In CD147-null mice, RPE cells transcribe mRNAs for MCT1, MCT3, and MCT4, but express no MCT protein (9). These results suggest that CD147 regulate MCT expression posttranscriptionally. However, no information is available on whether MCTs are required for the transcription or translation of CD147. To obtain this information, we generated pSuper-based siRNAs against human CD147 and MCT1 and studied their effect on the expression of the partner protein. Experiments were carried out in a subline of Caco2 human intestinal epithelial cells, C2BBE1, which express constitutively CD147 and MCT1, but do not express MCT4 protein. In agreement with the published observations in CD147-null mice, down-regulation of CD147 abrogated the expression of MCT1 in C2BBE1 cells (Fig.

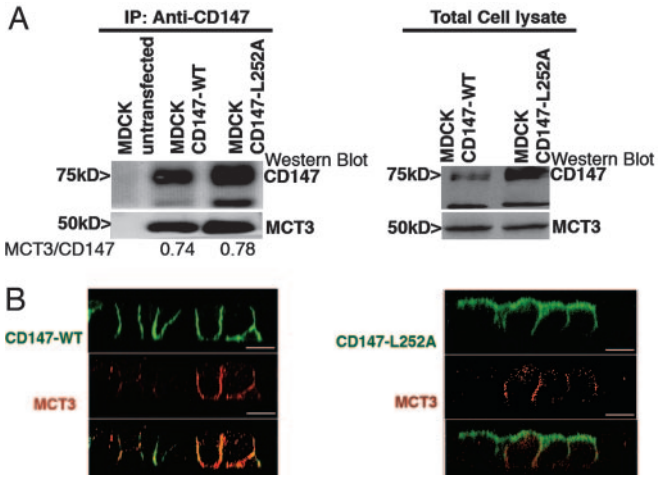

Fig. 3. CD147 does not regulate the polarized distribution of MCT3/CD147 complex. (*A*) Coimmunoprecipitation of CD147 and MCT3. MDCK stable clones (CD147-WT and CD147-L252A) were transfected with human MCT3. (*Left*) Immunoprecipitation with RET-PE2 Ab against rat CD147 followed by Western blot for MCT3 in the immunoprecipitate confirmed that the human MCT3 interacts with the rat CD147-WT and CD147-L252A. (*Right*) Western blot of total cell lysate. (*B*) LSCM of CD147 and MCT3. Clonal MDCK cell lines overexpressing GFP-tagged rat CD147 (WT or L252A mutant) were transfected with human MCT3. Shown are LSCM *x–z* sections of these MDCK cell lines immunostained for MCT3 (red) and CD147-WT (green) (*Left*) or CD147-L252A (green) (*Right*). (*Right*) Note that overexpression of apically targeted CD147-L252A did not affect the basolateral localization of MCT3. Similar to MCT4/CD147 complex, the basolateral pool of CD147-L252A forms complex with MCT3. (Scale bar, 10 μm.)

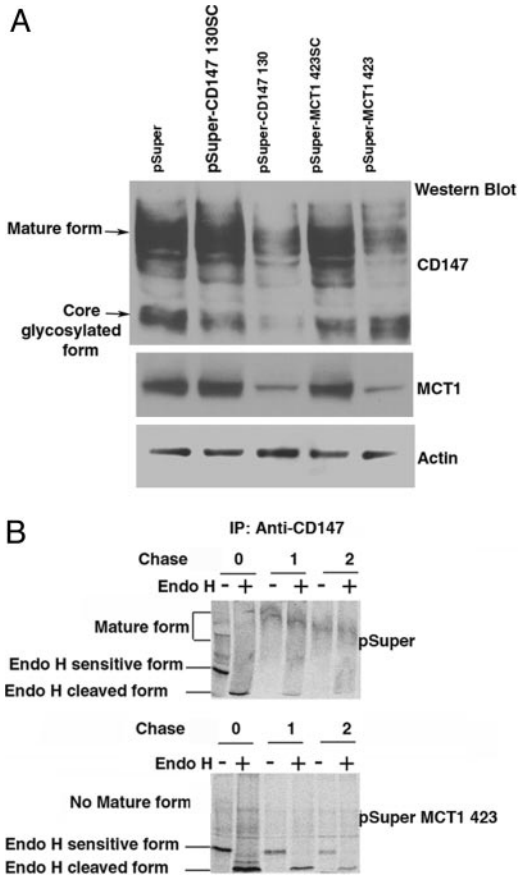

Fig. 5. MCT1 is essential for the maturation of CD147. (*A*) Western blot analysis of RNAi-treated Caco-2 cells. C2BBE, a subline of human Caco-2 cells, expresses both MCT1 and CD147 endogenously. Although these cells also express the MCT4 mRNA, we did not observe expression of MCT4 protein by Western blot (data not shown). CD147 and MCT1 were silenced by using pSuper vector-based siRNA. After transfection (72 h) of various pSuper constructs (pSuper, pSuper CD147130scrambled, pSuper CD147 130, pSuper MCT1 423scrambled, and pSuper MCT1 423), 20 μg of cell lysate was resolved by SDS/PAGE and analyzed by Western blot for the presence and levels of CD147 and MCT1. Protein levels were normalized against actin levels measured by a β-actin Ab. Note that down-regulation of CD147 led to concomitant reduction in the expression of MCT1 protein. Note also that silencing of MCT1 led to maturation arrest of CD147 in its core glycosylated form, demonstrating that MCT1 acts as a chaperone for CD147. (*B*) Pulse–chase analysis of RNAi-treated Caco cells. C2BBE1 cells transfected with either pSuper or pSuper-MCT1 423 plasmids were pulsed with [^{35}S]Met/Cys for 30 min and chased for 0, 1, and 2 h in the presence of excess cold amino acids. Immunoprecipitates obtained with human CD147 Ab were treated with Endo-H (+) or not (−), and the samples were analyzed by SDS/PAGE and analyzed by PhosphorImager (Molecular Dynamics). Control cells treated with empty pSuper vector show normal maturation of CD147 to Endo-H resistance within 1 h; only a small amount of immature Endo-H-sensitive form is seen at this time. In contrast, silencing of MCT1 hinders maturation of CD147 to Endo-H resistance. Under these conditions, Endo-H-sensitive CD147 is seen even after a 2-h chase.

5*A*). Interestingly, inhibition of the expression of MCT1 by siRNA resulted in apparent maturation arrest of CD147, as indicated by the accumulation of a core-glycosylated form of the protein and the disappearance of the mature, endoglycosidase-H (Endo-H)-resistant form of CD147 (Fig. 5*B*). pSuper-MCT1 321 and pSuper-MCT1 423 RNA interferences (RNAi), which are targeted to different regions of the mRNA of MCT1, were effective in inhibiting the expression of both MCT1 mRNA and protein. Both RNAi caused arrest in the maturation of CD147, but only the results obtained with pSuper-MCT1 423 RNAi are shown (Fig. 5). Pulse–chase analysis confirmed that suppression of MCT1 expression resulted in the accumulation of an Endo-H-sensitive form of CD147 (Fig. 5*B*). RT-PCR analysis did not detect any change in the mRNA transcripts of MCT1 and CD147, respectively, when CD147 and MCT1 were knocked down (Fig. 10, which is published as supporting information on the PNAS web site). These data suggest that the two subunits of the lactate transporter regulate each other post-transcriptionally, acting as bona fide cochaperones. The roles of MCT3 and MCT4 in the maturation of CD147 have not yet been characterized.

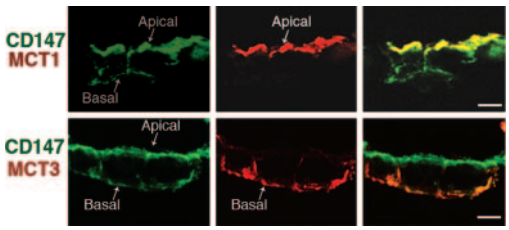

Fig. 4. Apical MCT1, basolateral MCT3, and predominantly apical CD147 in human fetal RPE. LSCM analysis of cryosection (8 μm) of polarized human fetal RPE cells grown on filters show apical localization of CD147 (green) and MCT1 (red) (*Upper*) and MCT3 (red) (*Lower*) colocalizing with basolateral pool of CD147 (green). (Scale bar, 10 μm.)

Discussion

Based on our previous demonstration that deletion of Leu-252 in the cytoplasmic domain of CD147 results in apical redistribution of this protein in MDCK cells (29), we developed an assay to identify the partner in the CD147/MCT heterocomplex that determines the polarized distribution of three different MCTs that play key roles in lactate and proton transport in kidney and retina. Our results provide new insights into the mechanisms that mediate the local-

CELL BIOLOGY

ization of MCTs in different epithelia. Our observations in MDCK cells indicate that MCT1 does not possess sorting signals, and CD147 is the dominant sorting partner that determines the basolateral localization of the MCT1-CD147 lactate transport complex. In RPE, endogenous CD147 and MCT1 are both expressed predominantly in the apical membrane (25, 28). As previous data from our laboratory demonstrate that the basolateral signal of CD147 is not recognized by RPE, resulting in its predominant apical localization (32), the MDCK experiments reported here strongly support a scenario in which the apical localization of MCT1 is determined by apically targeted CD147. In striking contrast, our MDCK data indicate that MCT3 and MCT4 have strong basolateral signals that are recognized by MDCK and RPE cells, thus explaining the basolateral localization of these transporters in both epithelia. Because MCT3 and MCT4 require CD147 for transport to the plasma membrane, it follows that a fraction of CD147 must be present at the basolateral membrane of MDCK and RPE cells. Indeed, this is what we observed in MDCK cells (Figs. 1–3) and in human fetal RPE cryosections (Fig. 4). Furthermore, previous biochemical studies from our laboratory involving domain-specific biotinylation of RPE in eye cups (28) and of stable MDCK cell lines expressing CD147 (ref. 29 and data in this report) demonstrate a sizeable fraction of this protein at the basolateral membrane of both cell types. Future work should identify a putative basolateral adaptor missing in RPE cells and the basolateral signals present in MCT3 and MCT4.

Here we have shown that a heterodimeric transporter, MCT1, relies on dominant sorting information in the glycosylated subunit for the polarized localization of the complex. A number of studies have identified dominant sorting signals in the nonglycosylated catalytic α-subunit in Na^+,K^+-ATPase and H^+,K^+-ATPase (33, 34) that are responsible for the basolateral or apical localization, respectively, of the heterodimeric pump. The basolateral localization of Na^+,K^+-ATPase is additionally stabilized by interactions of the α-subunit with ankyrin at the lateral membrane (35) and by interactions between neighboring β-subunits (36). We also show in this report that MCT3 requires CD147 for cell surface expression, as previously shown for MCT1 and MCT4 (9, 12). In addition, we demonstrate that the maturation of the glycosylated subunit CD147 into a Golgi form is completely dependent on the coexpression of MCT1 (Fig. 5). Together with previous results, our data suggests that coordinated regulation at the posttranslational level serves as a checkpoint in formation of a functional lactate transporter, as shown previously for Na^+ K^+ ATPase and potassium channels (37, 38, 39). Future studies should be conducted to address the role of MCT3 and MCT4 in the maturation of CD147.

Using our CD147-induced redistribution assay, we tested the hypothesis (17) that Glu-221 within the transmembrane domain of CD147 is responsible for the interaction with MCT and is therefore critically involved in plasma membrane delivery of both proteins. Our results reported here do not support this hypothesis. We demonstrate that mutation of Glu-221 to Ala (E221A) affects neither the surface expression of CD147 nor its association with MCT1, as assessed by the ability of the double mutant CD147-L252A-E221A to promote apical targeting of MCT1 (Fig. 9). It is not clear why different results are obtained by two different laboratories in this regard. Future studies are necessary to identify the CD147 domain that mediates interaction with MCTs.

In addition to lactate, MCTs also transport monocarboxylate compounds like acetic acid, propionic acid, pyruvic acid, and ketone bodies (6). Other studies implicate MCTs in the transport of drugs, such as salicylate, valproic acid, and atorvastatin, across the plasma membrane (40–42). A defect in lactate efflux by MCT1 has been associated with one rare condition known as cryptic exercise intolerance in humans (43). The importance of polarized targeting of transporters is underscored by diseases like autosomal dominant distal renal tubular acidosis, which may be caused by the loss of polarized targeting of the normally basolateral $Cl^-/HCO3^-$ exchanger AE1 (44), and autosomal nephrogenic diabetes insipidus may be caused by reversed polarity of an aquaporin-2 water channel (45). Thus, the paradigm for the study of polarized expression of lactate transporters introduced here has broad implications for the analysis of a variety of physiological, pharmacological, and pathological processes.

We thank Dena Almeida for technical assistance. This work was supported by National Institutes of Health Grants EY08538, EY012042, EY00444, EY00331, and GM34107; National Institutes of Health National Research Service Award EY14307 (to A.D.); the Charles and Margaret Dyson Chair in Ophthalmic Research (to E.R.B.); the Dolly Green Chair in Ophthalmology (to D.B.); and the Dyson Foundation.

1. Yeaman, C., Grindstaff, K. K., Hansen, M. D. & Nelson, W. J. (1999) *Curr. Biol.* **9,** R515–R517.
2. Rodriguez-Boulan, E., Kreitze, G. & Musch, A. (2005) *Nat. Rev. Mol. Cell Biol.* **6,** 233–247.
3. Keller, P. & Simons, K. (1997) *J. Cell Sci.* **110,** 3001–3009.
4. Dunbar, L. A. & Caplan, M. J. (2001) *J. Biol. Chem.* **276,** 29617–29620.
5. Verrey, F., Jack, D. L., Paulsen, I. T., Saier, M. H., Jr., & Pfeiffer, R. (1999) *J. Membr. Biol.* **172,** 181–192.
6. Halestrap, A. P. & Price, N. T. (1999) *Biochem. J.* **343,** 281–299.
7. Groves, J. D. & Tanner, M. J. (1992) *J. Biol. Chem.* **267,** 22163–22170.
8. Bauch, C., Forster, N., Loffing-Cueni, D., Summa, V. & Verrey, F. (2003) *J. Biol. Chem.* **278,** 1316–1322.
9. Philp, N. J., Ochrietor, J. D., Rudoy, C., Muramatsu, T. & Linser, P. J. (2003) *Invest. Ophthalmol. Vis. Sci.* **44,** 1305–1311.
10. Halestrap, A. P. & Meredith, D. (2004) *Pflugers Arch.* **447,** 619–628.
11. Price, N. T., Jackson, V. N. & Halestrap, A. P. (1998) *Biochem. J.* **329,** 321–328.
12. Kirk, P., Wilson, M. C., Heddle, C., Brown, M. H., Barclay, A. N. & Halestrap, A. P. (2000) *EMBO J.* **19,** 3896–3904.
13. Carpenter, L., Poole, R. C. & Halestrap, A. P. (1996) *Biochim. Biophys. Acta* **1279,** 157–163.
14. Yoon, H., Fanelli, A., Grollman, E. F. & Philp, N. J. (1997) *Biochem. Biophys. Res. Commun.* **234,** 90–94.
15. Poole, R. C. & Halestrap, A. P. (1993) *Am. J. Physiol.* **264,** C761–C782.
16. Garcia, C. K., Goldstein, J. L., Pathak, R. K., Anderson, R. G. & Brown, M. S. (1994) *Cell* **76,** 865–873.
17. Wilson, M. C., Meredith, D. & Halestrap, A. P. (2002) *J. Biol. Chem.* **277,** 3666–3672.
18. Stockinger, H., Ebel, T., Hansmann, C., Koch, C., Majdic, O., Prager, E., Patel, D. D., Fox D. A., Horejsi, V., Sagawa, K. & Shen, D. (1997) in *Leucocyte Typing VI*, eds. Kishimoto, T., Kikutani, H., von dem Born, A. E. G. K., Goyert, S. M., Miyasaka, M., Moretta, L., Okumura, K., Shaw, S., Springer, T. A., Sugamura, K. & Zola, H. (Garland, New York), pp. 760–763.
19. Wilson, M. C., Meredith, D., Fox, J. E., Manoharan, C., Davies, A. J. & Halestrap, A. P. (2005) *J. Biol. Chem.* **280,** 27213–27221.
20. Porras, O. H., Loaiza, A. & Barros, L. F. (2004) *J. Neurosci.* **24,** 9669–9673.
21. Pellerin, L., Halestrap, A. P. & Pierre, K. (2005) *J. Neurosci. Res.* **79,** 55–64.
22. Poitry-Yamate, C. L., Poitry, S. & Tsacopoulos, M. (1995) *J. Neurosci.* **15,** 5179–5191.
23. Hori, K., Katayama, N., Kachi, S., Kondo, M., Kadomatsu, K., Usukura, J., Muramatsu, T., Mori, S. & Miyake, Y. (2000) *Invest. Ophthalmol. Vis. Sci.* **41,** 3128–3133.
24. Igakura, T., Kadomatsu, K., Kaname, T., Muramatsu, H., Fan, Q. W., Miyauchi, T., Toyama, Y., Kuno, N., Yuasa, S., Takahashi, M., *et al.* (1998) *Dev. Biol.* **194,** 152–165.
25. Philp, N. J., Yoon, H. & Grollman, E. F. (1998) *Am. J. Physiol.* **274,** R1824–R1828.
26. Philp, N., Chu, P., Pan, T. C., Zhang, R. Z., Chu, M. L., Stark, K., Boettiger, D., Yoon, H. & Kieber-Emmons, T. (1995) *Exp. Cell Res.* **219,** 64–73.
27. Philp, N. J., Wang, D., Yoon, H. & Hjelmeland, L. M. (2003) *Invest. Ophthalmol. Vis. Sci.* **44,** 1716–1721.
28. Marmorstein, A. D., Bonilha, V. L., Chiflet, S., Neill, J. M. & Rodriguez-Boulan, E. (1996) *J. Cell Sci.* **109,** 3025–3034.
29. Deora, A. A., Gravotta, D., Kreitzer, G., Hu, J., Bok, D. & Rodriguez-Boulan, E. (2004) *Mol. Biol. Cell.* **15,** 4148–4165.
30. Brummelkamp, T. R., Bernards, R. & Agami, R. (2002) *Science* **296,** 550–553.
31. Rosenberg, S. O., Fadil, T. & Schuster, V. L. (1993) *Biochem. J.* **289,** 263–268.
32. Marmorstein, A. D., Gan, Y. C., Bonilha, V. L., Finnemann, S. C., Csaky, K. G. & Rodriguez-Boulan, E. (1998) *J. Cell Biol.* **142,** 697–710.
33. Muth, T. R., Gottardi, C. J., Roush, D. L. & Caplan, M. J. (1998) *Am. J. Physiol.* **274,** C688–C696.
34. Dunbar, L. A., Aronson, P. & Caplan, M. J. (2000) *J. Cell Biol.* **148,** 769–778.
35. Nelson, W. J. & Veshnock, P. J. (1987) *Nature* **328,** 533–536.
36. Shoshani, L., Contreras, R. G., Roldan, M. L., Moreno, J., Lazaro, A., Balda, M. S., Matter, K. & Cereijido, M. (2005) *Mol. Biol. Cell.* **16,** 1071–1081.
37. Jaunin, P., Horisberger, J. D., Richter, K., Good, P. J., Rossier, B. C. & Geering, K. (1992) *J. Biol. Chem.* **267,** 577–585.
38. Geering, K., Beggah, A., Good, P., Girardet, S., Roy, S., Schaer, D. & Jaunin, P. (1996) *J. Cell Biol.* **133,** 1193–1204.
39. Ma, D. & Jan, L. Y. (2002) *Curr. Opin. Neurobiol.* **12,** 287–292.
40. Hosoya, K., Kondo, T., Tomi, M., Takanaga, H., Ohtsuki, S. & Terasaki, T. (2001) *Pharm. Res.* **18,** 1669–1676.
41. Utoguchi, N. & Audus, K. L. (2000) *Int. J. Pharm.* **195,** 115–124.
42. Wu, X., Whitfield, L. R. & Stewart, B. H. (2000) *Pharm. Res.* **17,** 209–215.
43. Fishbein, W. N. (1986) *Science* **234,** 1254–1256.
44. Devonald, M. A., Smith, A. N., Poon, J. P., Ihrke, G. & Karet, F. E. (2003) *Nat. Genet.* **33,** 125–127.
45. Kamsteeg, E. J., Bichet, D. G., Konings, I. B., Nivet, H., Lonergan, M., Arthus, M. F., van Os, C. H. & Deen, P. M. (2003) *J. Cell Biol.* **163,** 1099–1109.
46. Le Bivic, A., Quaroni, A., Nichols, B. & Rodriguez-Boulan, E. (1990) *J. Cell Biol.* **111,** 1351–1361.